Dissolution of Mo/Al Bilayers in Phosphoric Acid

In Sung Kim,[†] Seung whan Chon,[‡] Ky Sub Kim,[†,‡] and Il Cheol Jeon[†,*]

[†]*Department of Chemistry, Chonbuk National University, Chonbuk 561-756, Korea*
[‡]*Research Center, Dongwoo Fine-Chem Co., LTD., Chonbuk 570-140, Korea*
Received August 16, 2003

In the phosphoric acid based etchant, the dissolution rates of Mo films were measured by microgravimetry and the corrosion potentials of Mo and Al were estimated by Tafel plot method with various concentrations of nitric acid. Dissolution rate of Mo increased with the nitric acid concentration and reached a limiting value at high concentration of nitric acid in ambient condition. Corrosion potentials of Mo and Al shifted to positive direction and the difference between potentials of both metals was about 1,100 mV and 1,200 mV with 1% and above 4% of HNO_3, respectively. For a Mo/Al bilayers, the dissolution rate inversion is the main reason for good taper angle in shower etching process. Taper angles are observed by scanning electron microscope (SEM) after wet etching process for Mo/Al layered films with different concentrations of HNO_3. In the etch side profile, it was found that Al corroded faster than Mo below 4% of HNO_3 in dip etching process, however, Mo corroded faster above 4%. Trend for variation of taper angle of etched side of Mo/Al layered film can be explained by considering the effect corrosion rates of both metals with various concentrations of HNO_3.

Key Words : Wet etching, Tafel plot, Quartz crystal microbalance, SEM, HNO_3

Introduction

The etching processes are very important for the semiconductor and liquid crystal display (LCD) industries. Especially for the LCD makers the etching of metal layers is critical because the taper angle generated after the etching process should be satisfied with a suitable value. For this reason it might be a key to the etching process to understand about the metal dissolution.[1] In the case of the phosphoric acid based etchant, the dip etching of the Mo/Al bilayers used in the thin film transistor LCD manufacturing[2] yields positive taper angles, however, negative angles in the shower etching.[3] In order to understand the variation of the taper angles according to the etching method, it is required to know well about the dissolution reactions of Mo and Al and the mechanism of dissolution of Mo/Al bilayers. The corrosion at the metal bilayers was affected by the Galvanic corrosion which might be the main cause for the variation of the taper angles during the etching process.

In a previous report,[4] it was possible to control the taper angle by varying the nitric acid concentration in Cr/Cr-Mo bilayer etching process. The corrosion potentials and corrosion rates for Mo and Al were measured as a function of nitric acid content in the phosphoric acid base to understand the taper angle of Mo/Al bilayers. In this article we present an explanation for the taper angle variation in terms of the mixed potential and the nitric acid concentration effect on the corrosion rate.

Experimental Section

A commercial potentiostat (BAS 100B/W) was used to measure corrosion potentials. To prepare working electrodes, high purity (99.99%, Nilaco) molybdenum and aluminum rods (diameter, 3 mm; height, 5 mm) were inserted in the center of Teflon rods (diameter, 1 cm; height, 5 cm) to seal with Torr-Seal (Varian). The working electrodes were polished with sandpaper, alumina powder and then treated in an ultrasonicator just before each experimental run. To get Tafel plots, linear sweep voltammetry was performed at the scan rate of 5 mV s^{-1} with respect to a reference electrode (Pt wire).

A commercial quartz crystal microbalance(QCM, SHIn EQCN 1000) was used in the measurement of corrosion rates. For this purpose, the quartz crystal electrodes (10 MHz) with a Mo layer of 1500 Å deposited on a quartz disk (diameter, 14 mm) were used. The frequency change of 1 Hz is equivalent to 0.043 Å for molybdenum.

For the corrosion experiments, concentrated acids such as phosphoric acid (85%), nitric acid (70%), and acetic acid (99.9%) were supplied from Dongwoo Fine-Chem Co. to make up the corrosion solutions. The electrolyte solutions were prepared with de-ionized water (resistivity > 18 MΩ cm).

To begin the corrosion rate measurement using a QCM, the frequency fluctuation has to be smaller than 5 Hz. At first, the quartz crystal electrode was contacted with a solution in which the concentration of phosphoric acid was identical with the injection solutions containing various amount of nitric acid. When the frequency is stable enough for the experiment, the injection solution was injected to initiate the dissolution. The mass decrease due to corrosive dissolution was monitored as a function of time. The moment of injection was set to t = 0. After for a while, the frequency changed linearly when the concentration of nitric acid at the metal surface became high enough. In this work,

[*]Corresponding author. e-mail: icjeon@moak.chonbuk.ac.kr

Table 1. Corrosion potentials of the metal electrodes of Mo and Al as a function of nitric acid concentration

Corrosion Potential, V								
Metal	Mo				Al			
temperature	room temp.		30 °C		room temp.		30 °C	
conc. HNO_3, %	aerated	deaerated	aerated	deaerated	aerated	deaerated	aerated	deaerated
0.5	-0.40	-0.41	-0.58	-0.59	-1.48	-1.50	-1.51	-1.50
1.0	-0.36	-0.37	-0.57	-0.56	-1.47	-1.46	-1.44	-1.46
2.0	-0.33	-0.34	-0.52	-0.53	-1.43	-1.41	-1.39	-1.42
3.0	-0.30	-0.30	-0.45	-0.49	-1.42	-1.39	-1.37	-1.44
4.0	-0.18	-0.24	-0.32	-0.38	-1.39	-1.39	-1.38	-1.40
5.0	-0.16	-0.16	-0.29	-0.29	-1.39	-1.37	-1.36	-1.40
6.0	-0.16	-0.16	-0.28	-0.29	-1.38	-1.37	-1.33	-1.37
7.0	-0.17	-0.17	-0.31	-0.31	-1.37	-1.36	-1.36	-1.41
7.8	-0.18	-0.18	-0.32	-0.32	-1.37	-1.37	-1.40	-1.42

the slope at linear frequency change was defined to be the corrosion rate.

Mo/Al double layers were prepared on glass substrates using DC magnetron. Scanning electron microscopes (SEM, Hitachi S-4200 or S-4700) were utilized to monitor the taper angles after corrosion of thin metal layers.

Results and Discussion

Polarization curves: Corrosion potential shift vs. Nitric Acid concentration. All the experiments were performed in solutions containing a constant amount of phosphoric acid with variable concentration of nitric acid. The overall data of corrosion potential are represented in Table 1. As shown in the redox polarization curves (Fig. 1), the corrosion potential of Mo shifts to the positive direction with the increase of the nitric acid concentration. The shift is nearly constant when the concentration is higher than 4%, which is summarized in Figure 2. The reduction current density attributed to the hydrogen evolution also increases with the nitric acid concentration. On the other hand, the oxidation current density decreases as the passivated layers are getting thicker with the nitric acid concentration. As for Al metal, the corrosion potential shifts to the positive direction in the

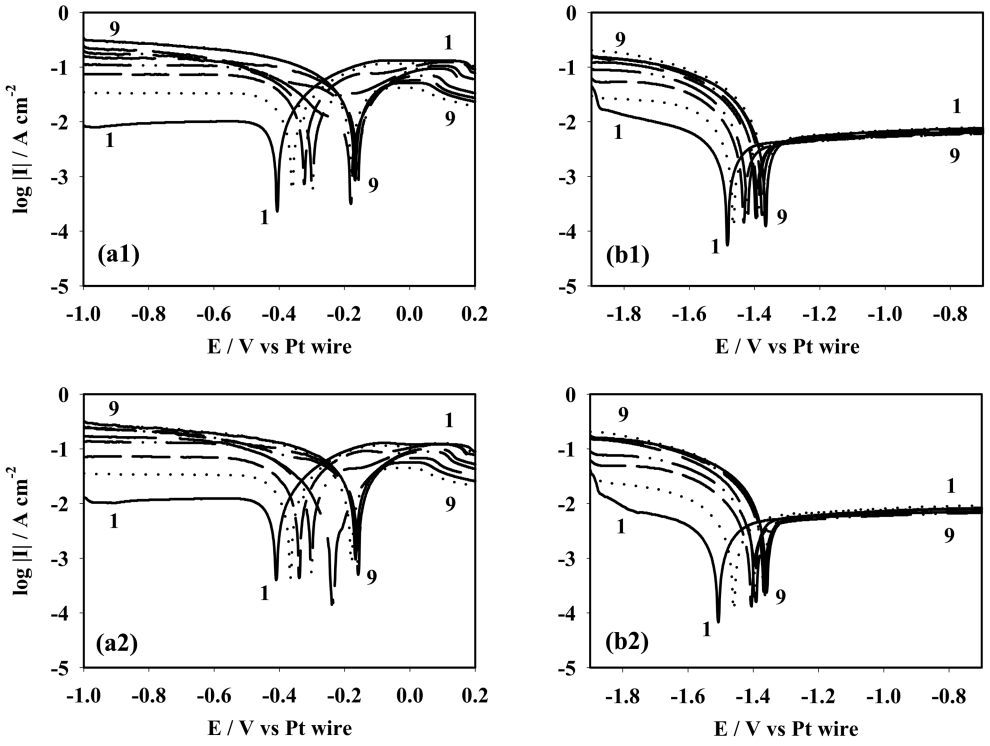

Figure 1. Effect of nitric acid concentration on the anodic and cathodic polarization response of Mo (a) and Al (b) in aerated (a1), (b1) and deaerated (a2), (b2) phosphoric acid at a scan rate of 5 mVs^{-1} and room temperature when stirred; 1) 0.5%, 2) 1.0%, 3) 2.0%, 4) 3.0%, 5) 4.0%, 6) 5.0%, 7) 6.0%, 8) 7.0%, 9) 7.8%.

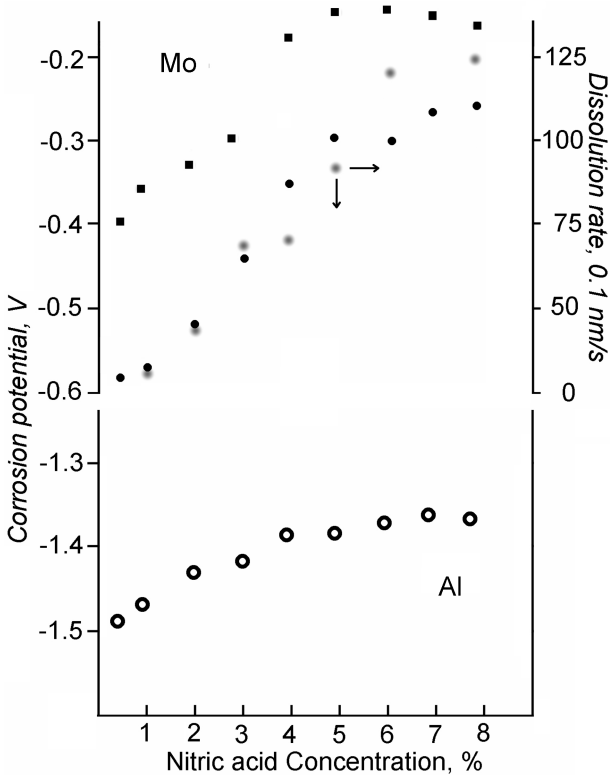

Figure 2. Effect of concentration of nitric acid on corrosion potentials of Mo(filled) and Al(empty) in phosphoric acid, ●○ at deaerated ambient condition. ■ at 30 °C. Blurred circle means dissolution rate.

lesser extent compared with that for molybdenum case. Unlike the Mo case, the oxidation current density does not change much with the nitric acid concentration as shown in Figure 1(b1). It is attributed to the formation of the passivated layer with a considerable thickness which prevents further passivation independent of the nitric acid concentration that means that the dissolution rate is slower than the electron transfer kinetics and it is rate-determining in the high concentration range. The deaerated cases purged with Ar gas are shown in Figure 1(a2) and (b2). The polarization curves are almost identical with those of the aerated cases and the corrosion potential difference is negligible. Summarily, the corrosion potentials of Mo and Al shift to positive potential in the more concentrated nitric acid and the effect is outstanding in Mo compared with that in Al. Generally, the corrosion potential shift to positive potential is equivalent to the acceleration of oxidation. At room temperature the corrosion potentials of Mo and Al shifted to the positive direction and the difference between the corrosion potentials of the two metals were about 1,100 and 1,200 mV at 1% and the concentration higher than 4% in nitric acid, respectively.

Corrosion rate: Current density. The current density of the anodic side of the Tafel plots reflects the rate of corrosion or oxidation, which is an exponential function of the overpotential (η), $e^{-a\eta}$. However, the actual corrosion rate will be limited by the kinetic parameters such as the dissolution rate. To understand the corrosion of two dissimilar metals contacted with each other in an etching solution, a schematic diagram is constructed based on the polarization curves explained previously. It is Figure 3 showing the anodic and cathodic potential-current curves for the dissolution of Al and Mo in the phosphoric acid based etchant. In the presence of nitric acid in the etchant, upper ones are the potential-current curves for Al and Mo, respectively. In the anodic region, metals dissolve along with oxidation. Lower ones are the virtual partial potential-current curves for the reduction of nitric acid. In the reduction reaction, hydrogen ions are reduced to evolve hydrogen gas which occurs at the surface of both metals.

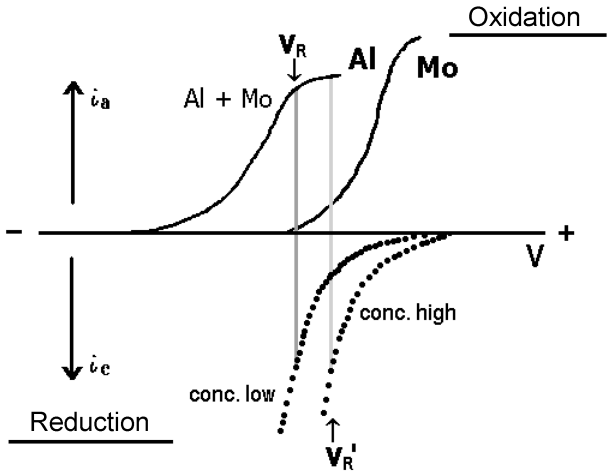

Figure 3. Schematic Diagram showing the mixed potentials in corrosion of the metal bilayers.

When two metals are electrically connected, the combined polarization curves for the oxidation and reduction reactions have to be considered. The Fermi levels of two metals become equal, hence, the electrons flow from the metal with the lower work function to that with higher one.[5] Considering the anodic current density or etching rate varies as an exponential function of overpotential, the potential-current curve for the bimetal case can be regarded to be similar with that of the lower work function that is Al in the present work meanwhile the mixed potential[6] of the bimetallic system assumes new values V_R and V_R' depending on the nitric acid concentration. The resulting mixed potentials for the bimetal case, V_R and V_R', are more positive than that for pure Al and more negative than that for pure Mo. Thus, it is clear that the contact between two metals has caused an increase in the etching rate of the less noble metal Al and a decrease in the etching rate of the nobler metal Mo.[7]

It is worthy to recall that the oxidation current density for Al (Fig. 1) does not change much with the nitric acid concentration, which can be considered equivalent to that the oxidation current density does not change much with the potential in the examined range of nitric acid concentration. It seems obvious that the corrosion or dissolution of Al in this potential range (or concentration range) is kinetically

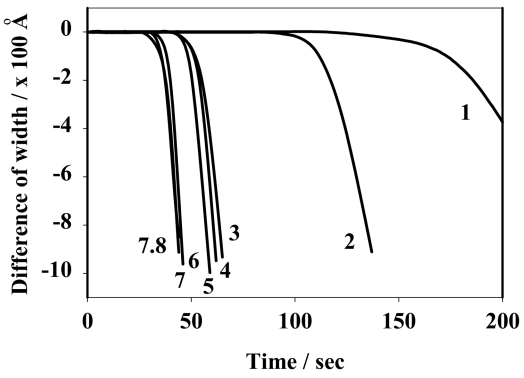

Figure 4. Corrosion rates of Mo with concentration of nitric acid in phosphoric acid under room temperature.

Table 2. Dissolution rates of Mo in various concentration of nitric acid

concentration/%	corrosion rate/Å s^{-1}
1.0	11.02
2.0	36.26
3.0	69.47
4.0	70.52
5.0	88.98
6.0	118.75
7.8	124.37

limited though it is not clear if the limitation is due to the formation of the passivated layer or not.

Stirring of the solution results in little potential shift to the positive direction for Mo while that of Al does not change at all or very little to the negative direction. It means that the mixed potential moves to the positive direction resulting in acceleration of corrosion for the Mo layer. From this finding, it is possible to expect that the shower etching will be faster than the dip etching due to the increased overpotential. Moreover, stirring helps to remove the bubbles on the metal surface which lets sustaining supply of the etching solution and enhances formation and dissolution of the metal oxides on the metal surface. Consequently it will provide the maximum ability for corrosion of the metal. When the solution is not stirred, the measured corrosion potential fluctuates which is due to bubbles formed more with the nitric acid concentration. Actually it was not easy to record Tafel plots when the solution was not stirred especially at high concentration. For this reason, the corrosion potentials exhibited in Figure 1 are only those measured while stirring.

As shown in Table 1, there is almost no difference in the polarization characteristics regardless of the presence of oxygen at both temperature conditions. It can be explained easily that the main constituents of the etching solutions are oxoacids with several oxygen atoms in the molecule, thus, the presence of oxygen in the solution does not affect much on the corrosion behavior of the etchants.

In order to understand the corrosion rate quantitatively, a QCM was used to measure the corrosive mass change.[8] The mass loss rate is obtained by the slope of the mass curve when the mass change becomes linear with time. The QCM cell was filled with the etchant solution except nitric acid and the oscillating frequency was monitored until sufficient stabilization. When the frequency was stabilized enough, a small volume of nitric acid to make up the designated concentration was added with much caution not to stir the etchant solution. The frequency change was measured to estimate the corrosion rate. In the initial stage of dissolution shown in Figure 4, the mass does not change much which is regarded as the mixing period after injection. As nitric acid diffuses, the dissolution rate increases gradually and then shows a constant slope at last. It obviously corresponds to the increase of mass loss rate due to increase of surface concentration of nitric acid. The dissolution rate measured by QCM is given in Table 2. The measured rates are exhibited in Figure 2 as the dissolution rate vs. nitric acid concentration. With the increase of the nitric acid concentration, the mixing period becomes shorter. The corrosion rate increases linearly with the concentration up to over 6% and it seems that the corrosion rate approaches a limiting value at higher concentration. In the concentration range studied in this article, the dissolution rate can be considered to change linearly with time and it is very similar to the trend of the corrosion potential change shown in Figure 2. It is explained that the formation of the metal oxide layers would be the rate determining step for the corrosion of metals at low concentration of nitric acid. At high concentration, however, the metal oxide formation gets sufficiently fast, then the dissolution rate will be the limiting factor.

Taper angle. As can be seen in Figure 5, the corrosion rate of Mo at low concentration of nitric acid is slow but that of Al is fast. The corrosion of the bilayer of Mo/Al is expected correspondingly to yield the undercuts of reverse taper angle. On the contrary, at high concentration the oxidation current density for Mo increases while that for Al is limited as described just above. That is because the mixed potential moves to the positive direction as the nitric acid content increases. Then the dissolution of Mo is much accelerated with the increased overpotential but the dissolution of Al is kinetically limited because of quite high overpotential.

Figure 5 shows the cross-sectional views of the Mo/Al bilayers taken by SEM after wet-etching. When the nitric acid concentration is lower than 4%, Al corroded faster than Mo producing under-cuts while Mo corroded faster at higher concentration. It means that there is a potential where the corrosion rates of two metals inversed. At a concentration or higher than a certain value the corrosion rate of Mo surpass that of Al and below this concentration Al corroded faster than Mo. In the actual shower etching process, the good taper angle is obtained with the nitric acid concentration higher than 8% for the Mo/Al bilayer because of faster dissolution of the Mo layer. It means that the dissolution rate for Mo is faster than that of Al at higher than 8% and that for Al is faster oppositely at lower than 8%. In the dip etching process, two corrosion rate curves are estimated experimentally to cross at about 4%. It is expected that the shower etching process should adopt more concentrated etching

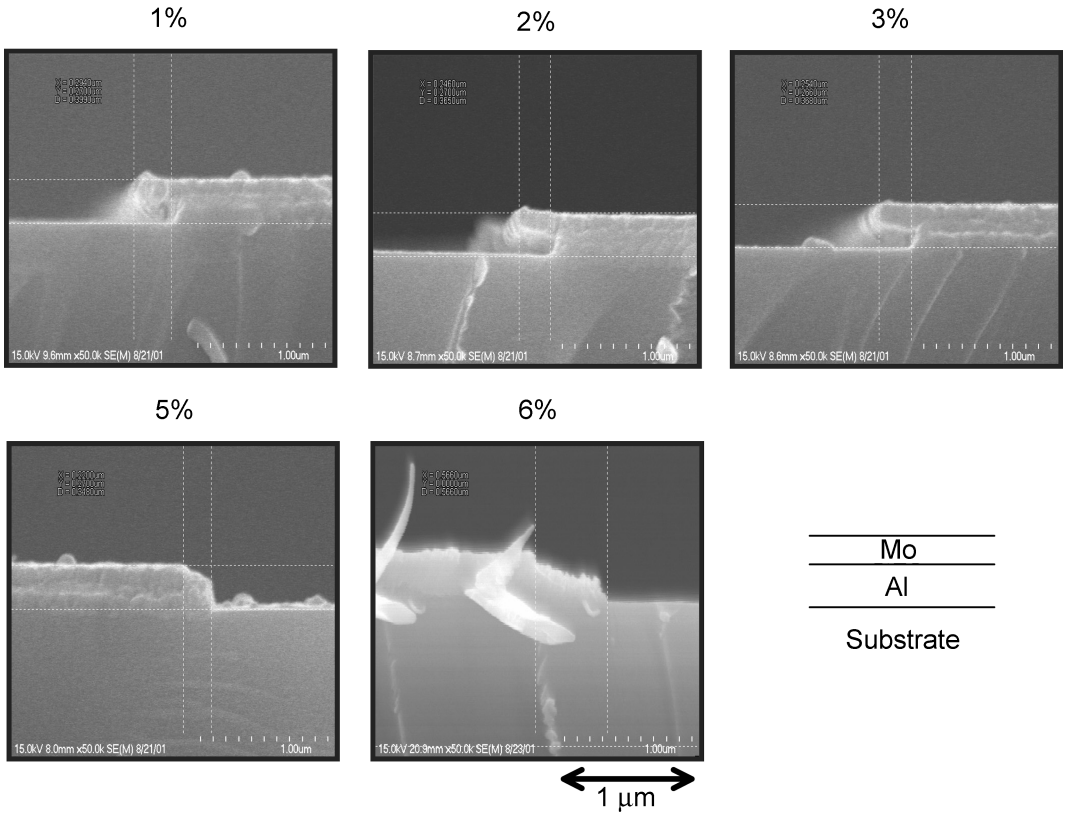

Figure 5. Cross sectional SEM image of wet etched Mo/Al layer at different HNO_3 concentration.

solution by 3-4% to produce good taper angles compared with the dip etching process.

Conclusions

In the concentrated phosphoric acid base etchant, the dissolution rate of Mo increased with the increase of the nitric acid content to approach a limiting rate at high concentration. At room temperature the corrosion potentials of Mo and Al shifted to the positive direction and the difference between the corrosion potentials of the two metals were about 1,100 and 1,200 mV at 1% and the concentration higher than 4% in nitric acid, respectively. When Mo and Al contacted each other, the dissolution of Mo is much accelerated with the increased corrosion potential but the dissolution of Al is kinetically limited because of high corrosion potential. This effect in the Mo/Al bilayer was greater in spray etching than in dip etching. Regarding the taper angle of the Mo/Al bilayer after the dip etching process, Al corroded much below 4% of nitric acid content and Mo dissolved faster over 4%.

Acknowledgment. We are grateful to Dongwoo Fine-Chem for the research fund and one of authors (ISK) acknowledges KOSEF for the financial support through 2001 internship program.

References

1. Kelly, J. J. *Electrochemistry of III-V Materials. A Review. Part I, Electrochemistry of Metal Dissolution*, *Nat. Lab. Report* **1981**, 5684.
2. Arai, T.; Makita, A.; Hiromasu, Y.; Takatsuji, H. *Thin Solid Films* **2001**, *383*, 287.
3. Tsujimura, T.; Kitahara, H.; Mikita, A.; Fryer, P.; Batey, J. *Conference Record of International Display Research Conference* **1994**, 424.
4. Kaneko, T.; Hashimoto, Y.; Ono, K.; Fujii, K.; Onisawa, K. *The 198th Meeting of The Electrochemical Society* **2000**, 780.
5. Schmickler, W. *Interfacial Electrochemistry*; Oxford University Press: 1996.
6. Oldham, H. B.; Myland, J. C. *Fundamentals of Electrochemical Science*; Academic Press: 1994.
7. Meerakker, van den J. *Wet Etching, Nat. Lab. Unclassified Report* **2002**, 805.
8. Baek, Y.; Frankel, G. S. *J. Electrochem. Soc.* **2003**, *150*, B1.